Multiple Sensor Optical Thermometry System for Application in Clinical Hyperthermia

VICTOR A. VAGUINE, MEMBER, IEEE, DOUGLAS A. CHRISTENSEN, MEMBER, IEEE, JOE H. LINDLEY, AND THOMAS E. WALSTON

Abstract—**The thermometry system described is based upon the temperature dependence of the band edge absorption of infrared light in GaAs crystal. The design of the thermometry was completed, and the system was subjected to an extensive evaluation, including testing with tissue phantoms and microwave applicators. The system has up to 12 temperature sensors which are packaged in two basic probe configurations: a single-sensor probe with a length of 1.2 m and a diameter of 0.6 mm; and a four-sensor linear array probe with a length of 1.2 m, diameter of 1.1 mm, and spacing of 1.5 cm between adjacent sensors. Results of thermometry evaluation are presented, including data on automatic calibration, temperature accuracy and stability, and EMI protection.**

INTRODUCTION

THE laboratory and clinical investigation of hyperthermia has now progressed to a stage where the engineering components involved are critical to a careful evaluation of the technique. This includes the development of heat applicators (both electromagnetic and ultrasonic) which will produce reasonably well-defined and perhaps controllable heating patterns, and temperature monitoring systems which are accurate and convenient to use in the presence of the heat-inducing energy source [1]. This paper describes the development of a fiber optic temperature probe system intended for use during electromagnetically induced hyperthermia.

When electromagnetic energy is employed to heat the treated region, temperature measurement problems may be encountered if traditional temperature probes, such as thermocouple wire pairs or thermistors with leads, are immersed in the fields while the power is on. This is due to the finite conductivity of the wires leading to the sensor and, to a lesser degree due to its small size, the conductivity of the sensor itself.

In order to eliminate or reduce interference errors, "nonperturbing" temperature probes have been designed. Development of these "nonperturbing" probes has followed two paths: 1) a thermistor as sensor in combination with high-resistance lead wires such as carbon-impregnated plastic, investigated by Bowman [2] and Larsen [3], and 2) optical fibers, either glass or plastic, as leads attached to an optical temperature sensor. A variety of optical sensors have been investigated, each technique possessing its particular advantages: Cetas [4] has explored the use of a birefringent crystal whose optical rotation changes with temperature; a liquid crystal sensor has been pursued by Rozzell [5] and Johnson [6]; and fluorescent sensors have been developed by Wickersheim [7] and by Samulski [8].

The fiber optic probe system described in this paper is based upon another type of optical sensor. It uses a small crystal of the semiconductor gallium arsenide (GaAs) whose optical absorption at a specifically chosen wavelength is sensitively related to the crystal's temperature [9]. The amount of optical signal returned after passage through the sensor may be detected and electronically translated, after calibration, into an indication of the probe's temperature. Details of the optical processes involved in the semiconductor sensor are discussed.

SEMICONDUCTOR/FIBER OPTIC TEMPERATURE MEASUREMENT TECHNIQUE

Semiconductor materials owe their unique conduction properties to the nature of the allowed electron energy states. What differentiates semiconductors from insulators and conductors is the forbidden energy gap E_g between the allowed energy bands. For semiconductors to be useful as an optical sensor, the energy gap E_g should satisfy the following condition:

$$kT \ll E_g;$$

thus, very few electrons have enough thermal energy to be excited across the energy gap.

When light is passed through the semiconductor material, photon energy may be sufficient to excite valence band electrons into the conduction band upon collision between the photons and the plentiful valence band electrons; thus the colliding photons are absorbed in the process. A sharp rise in photon absorption occurs when the photon energy exceeds the gap energy. This phenomenon is known as "band edge" absorption in semiconductor. Experimentally, it has been found that the absorption coefficient follows an exponential curve near the threshold wavelength $\lambda_g = hc/E_g$ in accordance with Urbach's rule [10]. This variation in attenuation versus wavelength is shown in Fig. 1 where light transmission through a 250 μm thick sample of GaAs is plotted as a function of optical wavelength at two temperatures, 25°C and 40°C. The band edge is shifted toward longer wavelengths as temperature increases, yielding a negative temperature coefficient.

This temperature behavior has been exploited for temperature sensor development based on the transmission of narrow-band optical radiation with its central wavelength situated

Manuscript received March 1, 1983; revised July 15, 1983.

V. A. Vaguine, J. H. Lindley, and T. E. Walston are with Clini-Therm Corporation, Dallas, TX 75243.

D. A. Christensen is with the University of Utah, Salt Lake City, UT 84112.

0018-9294/84/0100-0168$01.00

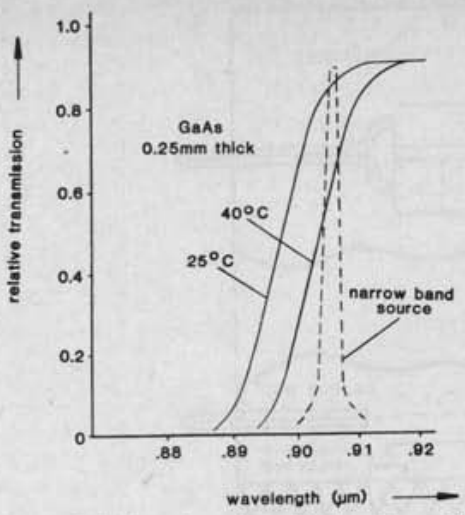

Fig. 1. The optical absorption edge of GaAs at two different temperatures (solid line). The dashed line shows the spectrum of a narrow-band source.

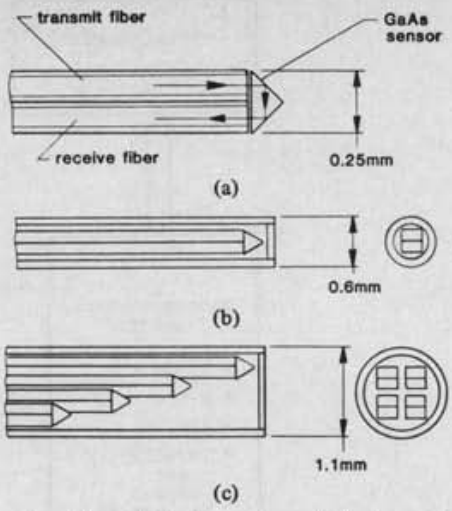

Fig. 2. Configuration of single- and multiple-temperature probes. (a) The semiconductor sensor and its attachment to the optic fibers. (b) Single sensor temperature probe. (c) Four-sensor temperature probe.

within the steep slope of the band edge. Fig. 1 shows the spectrum of such a source superimposed on the absorption curves.

Temperature Sensor Configuration

In our scheme, the optical radiation is transmitted to the sensor by one of a pair of small-diameter plastic fibers. The sensor is shaped in the form of a retroflector prism whereby the radiation which passes through the sensor is collected by the other fiber of the pair. Fig. 2(a) shows the configuration and dimensions of the sensor design. This arrangement of separate transmit and receive fibers considerably simplifies the optical design of the source and detector module since it eliminates the requirement for beam splitters and lenses at the interface between the fibers and the source and detector. These optical components are often bulky, lossy, and difficult to align.

The conductivity of the semiconductor sensor is less by many orders of magnitude than that of a comparable metallic part. For example, resistivity of the intrinsic GaAs is $10^8\ \Omega\cdot$cm. The small sensor volume further reduces any effect of a mismatch between tissue and probe conductivities. After attachment, the sensor and fibers are sheathed in Teflon tubing whose inner diameter is 0.3 mm and outer diameter is 0.6 mm [see Fig. 2(b)]; the end of the tube is heat sealed with a tiny Teflon plug.

Plastic fibers are chosen for their small outer diameter (0.12 mm) and their flexibility compared to glass fibers. The large numerical aperture (NA = 0.58) reduces the effect of bending losses, i.e., the loss of optical power in the fiber produced by sharp bending of the fiber [11], which appears as a change in temperature to the electronics module. One disadvantage of plastic fibers is related to the relatively high optical loss at a center wavelength of 905 nm due to light absorption by a hydroxyl radical. As a result, the overall length of the probes is limited to approximately 1.2 m.

The base of the probe consists of an L-shaped metal housing which contains the LED source (light emitting diode) and the silicon photodetector (PD) associated with each probe.

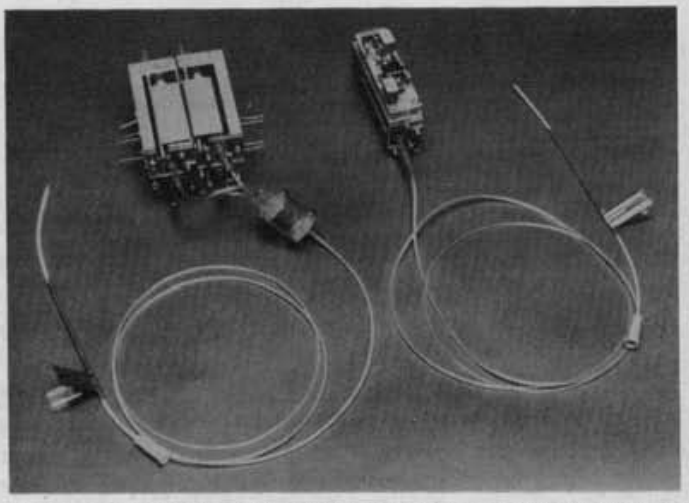

Fig. 3. Single sensor probe (left) and four-sensor linear array probe. Both are shown with their integrated module bases, closed end catheters, and hypodermic needles.

Fig. 3 shows a photograph of a single sensor probe with its base and a preamplifier PC board. The optical components are epoxied directly to the fiber ends; this integration of the fiber to the optical support devices substantially improves light transmission and decreases the optical losses. Compared to a previous design employing two metal fiber optic connectors per probe, this new integrated technique yields approximately 6-8 times more light power transmitted to the photodetector for a given length of probe, thus substantially improving signal-to-noise ratio, which can be translated into improvement of thermometry performance and increase of probe length.

The LED is a moderate-power GaAs LED, chosen to provide an appropriate center wavelength to match the absorption band edge at 0.905 μm. The transmit fiber is epoxied directly to the emitting surface of the LED after the protective cover has been removed; this maximizes transmitted power [12]. The receive fiber is placed against the photodetector window (as close as possible to the detection surface) and epoxied in place.

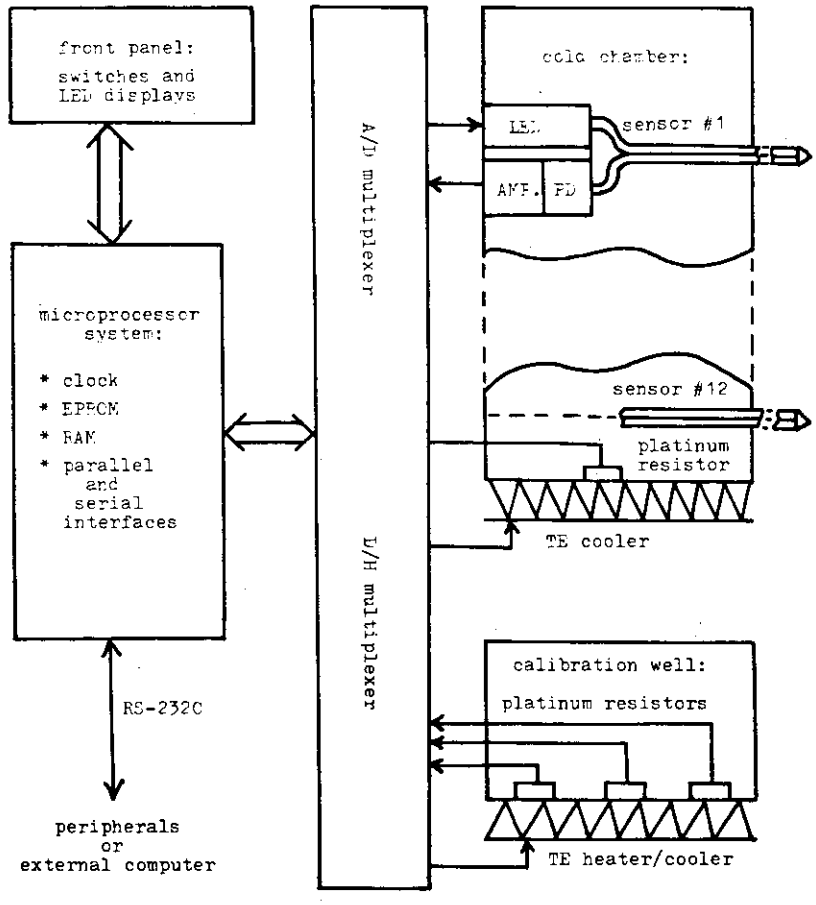

Fig. 4. A block diagram of the thermometry system.

The small total size of each sensor and its attached fibers has allowed us to develop a multiple-sensor probe, with several sensors arranged in a linear array inside a common sheathing tubing. Four-sensor arrays have been built with equal spacing of 1.0 or 1.5 cm between neighbor sensors. The four-sensor probe tubing has an inner diameter of 0.55 mm and an outer diameter of 1.1 mm [see Fig. 2(c)]. The base of this multiple sensor probe is a combination of individual bases, and can be installed in place of individual probes in the electronic console.

The module base of each probe is firmly attached to a temperature-controlled plate inside the electronics console, called a "cold chamber."

Thermometry Design and Functions

Early design of a single sensor probe, based on GaAs/fiber optic technique, has been developed by D. A. Christensen [9] and used initially as a part of a 433 MHz microwave hyperthermia system [13]. Here, we describe the latest design of the GaAs/fiber optic thermometry system with multiple sensor capability. A block diagram of the system is shown in Fig. 4. The major components include sensor modules, a cold chamber, a calibration well, microprocessor-based electronics, and a front panel with switches and digital displays.

The cold chamber is a thermally insulated housing with room for up to 12 sensor bases which are installed on a metal plate in the cold chamber.

It was found that the central wavelength and the spectrum of the emitted light by the LED are affected by temperature variations of the LED base. Therefore, temperature stabilization of the metal plate was provided in order to assure a high degree of stability in the light spectrum and the central wavelength during system operation. The temperature stabilization is achieved by the use of the microprocessor-based electronics with a platinum resistor as the temperature reference.

The microprocessor system is based on 8 bit Z80 CPU with a 12 Kbyte EPROM (electrically programmable read only memory) and an 8 Kbyte RAM (random access memory). Parallel interfaces are included for communication to other hardware in the system, and a serial RS-232C port handles all communications to external peripherals or computers. A second serial RS-232C port is available for future expansion.

Thermometry system functions fall naturally into two categories: basic temperature measurements and the operator interface (front panel and peripherals). The microprocessor system controls both functions.

Primary operator control of the thermometry system is through three dedicated switches and two digital displays on the front panel (Fig. 5). The power switch turns the system on and off. The calibration switch initiates an automatic calibration. By using the sensors select switch one can display temperature on the front panel for a selected sensor. The displays are bright LED's specifying the sensor number and its temperature.

The automatic calibration is accomplished by inserting all sensors into the calibration well and initiating the calibration

Fig. 5. An overall view of the thermometry system with 12 single-sensor temperature probes.

process. During this mode, the calibration well is initially cooled to less than 20°C and then warmed in 2-3° steps to approximately 55°C. At each step, the calibration well is held at a constant temperature long enough to accurately measure and store all sensor readings in RAM's, including temperature data from three high precision platinum sensors used as temperature references. The calibration process takes approximately 9 min and provides data necessary to measure temperature over the range of 20-55°C. The calibration data table is used to convert sensor readings (optical transmitted power) into temperature readings. During calibration, the progress on calibration is displayed on the front panel in terms of real time temperature of the calibration well. Part of the RAM memory, where calibration data is stored, is powered by a battery when the thermometry is unplugged from an external power line.

Although basic functions provided by the front panel control are sufficient to operate and monitor the system, peripherals, such as video display and printer, can be connected to RS-232C port in order to expand the monitoring capabilities into more sophisticated real-time, visual, audio, and hard copy forms for all sensors.

Performance and Clinical Application

The thermometry has been tested and evaluated, including measurements with tissue phantoms and microwave applicators.

Immediately after calibration, accuracy of all probes is within ±0.1°C. Temperature drift testing has indicated that to obtain absolute accuracy of ±0.2°C for all probes, calibration has to be performed within the last 8 h. The loss of accuracy after 8 h, however, is minimal, and even after two days of operation it approaches only ±0.3°C. Throughout the testing, it was common to observe several sensors reading within one hundredth of one degree of each other.

The system is essentially immune to EMI effect for the frequencies used in microwave hyperthermia. For example, using a well matched 915 MHz microwave applicator aimed directly at the thermometry system, no noticeable temperature reading effect was observed until microwave power density, measured at the thermometry, rose to a level of approximately 5 W/cm^2, which substantially exceeds any expected microwave stray radiation during hyperthermia treatment. The fiber optic probes experience no accuracy loss nor produce noticeable electromagnetic field perturbation in electromagnetic fields.

Accuracy of the probe readings can be affected if the probes are bent or pinched during temperature measurements. Testing has shown that a bend radius of 1 cm degrades accuracy by 0.1°. However, this effect was reversible once a probe was unbent. No appreciable effect was observed for radii greater than 2.5 cm. In clinical applications, it is doubtful that bend radii small enough to cause appreciable error will be required to place the probes at treatment sites. The bend effect means, rather, that care should be taken to avoid pinching or kinking the probes.

The multiple sensor (linear array) probe, since it consists of four sensors bundled together in one probe, was of special interest during testing. The individual sensors within the probe yielded accuracies of ±0.2°C after calibration. The key conclusion from this testing was that the bundling of multiple sensors together had no effect upon the basic fiber optic/GaAs crystal temperature measurement phenomenon. Small degradation of accuracy for the linear array is probably a result of a temperature gradient along the calibration well.

Key design features of both the thermometry system and accessories have combined to make it well suited to the clinical environment. The primary factors for clinical application such as accuracy, multiple point temperature measurement, automatic calibration, and operator system control/monitoring have been more than adequately addressed by the system's basic design. Other important factors relate to how the sensors must be handled, brought to the treatment site, and actually inserted.

The thermometry system is relatively small for a multiple probe system (19 cm high, 29 cm wide, and 50.8 cm long) so that it can be easily placed in close proximity to the patient. The sensor probe length of 1.2 m allows enough distance between system and patient for placement of probes at several different treatment sites. Almost half the length of each probe is covered with a Teflon sleeve for protection against rough handling. The probe tips, however, are delicate due to their small diameters and must be handled with care (see Figs. 2 and 3).

The clinical requirement for a simple but safe method of sensor inserting into living tissue has been met by the closed end catheter technique. For a single sensor probe this entails the use of a sterile 19 gauge closed end catheter and sterile 17 gauge breakaway hypodermic needle (16 gauge catheter and 14 gauge needle for the linear array). The catheter is first inserted into the needle to give it the sharp point and stiffness needed for proper placement of the needle/catheter at the correct site, angle, and depth. After insertion, the needle is split and withdrawn leaving the catheter in the tissue. The sensor can then be inserted into the catheter to implement temperature measurements.

Acknowledgment

The authors wish to express their appreciation to K. Chun for his advice and technical assistance.

References

[1] D. A. Christensen and C. H. Durney, "Hyperthermia production for cancer therapy: A review of fundamentals and methods," *J. Microwave Power*, vol. 16, pp. 89–105, 1981.

[2] R. R. Bowman, "A probe for measuring temperature in radio frequency-heated material," *IEEE Trans. Microwave Theory Tech.*, vol. MTT-24, pp. 43–45, 1976.

[3] L. E. Larsen, R. A. Moore, and J. Acevedo, "A microwave decoupled brain temperature transducer," *IEEE Trans. Microwave Theory Tech.*, vol. MTT-22, pp. 438–444, 1974.

[4] T. C. Cetas, "A birefringent crystal optical thermometer for measurements in electromagnetically induced heating," in *Proc. USNC/URSI Symp.* (Bur. Radiol. Health), Rockville, MD, 1975, C. C. Johnson and J. L. Shore, Eds.

[5] T. C. Rozzell, C. C. Johnson, C. H. Durney, J. L. Lords, and R. G. Olsen, "A nonperturbing temperature sensor for measurements in electromagnetic fields," *J. Microwave Power*, vol. 9, pp. 241–249, 1974.

[6] C. C. Johnson, O. P. Gandhi, and T. C. Rozzell, "A prototype liquid crystal fiberoptic probe for temperature and power measurements in RF fields," *Microwave J.*, vol. 18, pp. 55–59, 1975.

[7] K. A. Wickersheim and R. V. Alves, "Recent advances in optical temperature measurements," *Ind. Res. Develop.*, vol. 21, p. 82, 1979.

[8] T. Samulski and P. N. Shrivastava, "Photoluminescent thermometer probes: Temperature measurements in microwave fields," *Science*, vol. 208, pp. 193–194, 1980.

[9] D. A. Christensen, "A new nonperturbing temperature probe using semiconductor band edge shift," *J. Bioeng.*, vol. 1, pp. 541–545, 1977.

[10] J. I. Pankove, *Optical Processes in Semiconductors*. New York: Dover, 1975.

[11] D. Gloge, "Bending loss in multimode fibers with graded and ungraded core index," *Appl. Opt.*, vol. 11, pp. 2506–2513, 1972.

[12] K. H. Yang and J. D. Kingsley, "Calculation of coupling losses between light emitting diodes and low-loss optical fibers," *Appl. Opt.*, vol. 14, pp. 288–293, 1975.

[13] V. A. Vaguine, R. H. Giebeler, Jr., A. H. McEuen, and G. M. Hahn, "A microwave direct-contact applicator system for hyperthermia therapy research," in *Proc. 3rd Int. Symp. Cancer Therapy by Hyperthermia, Drugs, Rad.*, NCI Monograph 6, 1982, pp. 461–464.

Victor A. Vaguine (M'82) photograph and biography not available at the time of publication.

Douglas A. Christensen (M'69) photograph and biography not available at the time of publication.

Joe H. Lindley, photograph and biography not available at the time of publication.

Thomas E. Walston, photograph and biography not available at the time of publication.